

NOTES AND CORRESPONDENCE

Net Energy Dissipation Rates in the Tropical Ocean and ENSO Dynamics

ALEXEY V. FEDOROV

Department of Geology and Geophysics, Yale University, New Haven, Connecticut

(Manuscript received 14 November 2005, in final form 3 July 2006)

ABSTRACT

How unstable is the tropical ocean–atmosphere system? Are two successive El Niño events independent, or are they part of a continual (perhaps weakly damped) cycle sustained by random atmospheric disturbances? How important is energy dissipation for ENSO dynamics? These closely related questions are frequently raised in connection with several climate problems ranging from El Niño predictability to the impact of atmospheric “noise” on ENSO. One of the factors influencing the system’s stability and other relevant properties is the damping (decay) time scale for the thermocline anomalies associated with the large-scale oceanic motion. Here this time scale is estimated by considering energy balance and net energy dissipation in the tropical ocean and it is shown that there are two distinct dissipative regimes: in the interannual frequency band the damping rate is approximately $(2.3 \text{ yr})^{-1}$; however, in a near-annual frequency range the damping appears to be much stronger, roughly $(8 \text{ months})^{-1}$.

1. Introduction

The interplay between the tropical ocean and atmosphere produces the Southern Oscillation—the dominant mode of climate variability in the Pacific. Its warm phase (El Niño) is typically followed by the cold phase (La Niña), so that a continual, albeit irregular, oscillation is maintained (see Figs. 1–2). Numerous studies over the past two decades of the interactions between the tropical oceans and the atmosphere have advanced our understanding of El Niño and its associated phenomena enormously [see the June 1998 issue of the *Journal of Geophysical Research* (Vol. 103, No. C7) or the recent monograph by Wang et al. 2004]. ENSO is now understood as a natural mode of oscillation, attributable to tropical ocean–atmosphere interactions in which the winds create sea surface temperature gradients that in turn reinforce the winds, and to negative feedbacks involving the dynamical response of the ocean to changes in the winds.

Conceptually, El Niño is often described as an adiabatic, zonal redistribution of warm water from the west-

ern to the eastern equatorial Pacific in response to a relaxation of the easterly trade winds, followed by a meridional redistribution of mass between the narrow equatorial band and certain regions off the equator (as in the recharge–discharge oscillator of Jin 1997a,b). In reality, any oceanic motion and changes in the thermocline depth would entail energy dissipation due to turbulent mixing or energy loss at the basin boundaries, for example. This dissipation, although relatively small, may become critical for a number of important problems (see below). The main purpose of this study is to estimate the relative strength of such dissipative effects.

A persistent problem of climate theory and modeling is whether the ENSO cycle is self-sustained or damped (Fedorov and Philander 2000, 2001). If the tropical coupled system is strongly damped, then random atmospheric disturbances are responsible for initiation of each El Niño event and for maintaining the oscillation (for a discussion, see Fedorov et al. 2003; Philander and Fedorov 2003; Kessler 2002). On the other extreme, if the system is sufficiently unstable, a self-sustained oscillatory regime is possible. The problem is of direct relevance to El Niño prediction and modeling and to questions such as what controls El Niño amplitude, phase, duration, and irregularity. To address these issues one has to assess the stability properties of the coupled ocean–atmosphere system. This stability de-

Corresponding author address: Dr. Alexey Fedorov, Department of Geology and Geophysics, Yale University, P.O. Box 208109, New Haven, CT 06520.
E-mail: alexey.fedorov@yale.edu

depends on two main factors—the rate of damping of the ocean motion associated with the propagation of thermocline depth anomalies (e.g., Thompson and Battisti 2000, 2001) and the combined strength of positive feedbacks provided by ocean–atmosphere interactions (e.g., Dijkstra and Neelin 1995; Jin 1997a,b). The latter factor depends mostly on atmospheric processes and as such is not considered here. The focus of this study is the oceanic component of the problem, that is, the effective rate of damping of the large-scale oceanic motion—the damping rate directly related to energy dissipation in the tropical basin.

That the ocean damping is indeed important for ENSO dynamics was clearly demonstrated by Thompson and Battisti (2000, 2001) who used an intermediate coupled model to show that changes in damping rates can strongly affect the simulated spectrum of the interannual variability. In particular, when they increased the explicit damping coefficient in their model by some 40%, the characteristic period of simulated ENSO shifted from 3.5 to about 5 yr, and even more importantly the magnitude of the peak of the power spectrum decreased by almost an order of magnitude.

Lately, small-scale mixing processes in the ocean and their effect on climate have been attracting growing attention, with a particular emphasis on the relationship between mixing and the global overturning circulation (e.g., Wunsch and Ferrari 2004). The focus of this study is different—we will be evaluating the net damping of the slow large-scale thermocline depth anomalies and associated anomalies in the tropical circulation. A strict definition of the damping rates, based on the energetics and relevant to interannual climate variability, will be given in the next section.

2. The energetics of ENSO

In a series of recent publications, the energetics of ENSO have emerged as a promising perspective on the dynamics of ocean–atmosphere interactions (Goddard and Philander 2000; Fedorov et al. 2003; Fedorov 2002; also see Oort et al. 1989; Wunsch 1998). These studies of the energetics indicate that the rate of change of available potential gravitational energy in the tropical ocean is equal to the work done on the ocean by the wind (per unit time) minus dissipation and energy fluxes out of the domain. Thus, there is an approximate balance between the terms

$$dE/dt = W + \text{Dissipation}, \quad (1)$$

where t is time, E is the perturbation available potential energy (APE), and W is the perturbation wind work averaged over the tropical Pacific Ocean (here the

tropical basin is defined as 15°N–15°S, 130°E–85°W). To calculate the time series of E and W , one needs to know the oceanic density field ρ , the near-surface zonal velocity U , and the zonal wind stress τ as a function of time and space, all in the tropical domain (see appendix A). A simple interpretation of Eq. (1) is that energy is supplied to the ocean in the form of wind work that modifies the ocean circulation and buoyancy fluxes, thus creating or destroying the APE. A fraction of that wind work, however, is dissipated rather than being used for changing the APE.

The comprehensive paper of Goddard and Philander (2000) was the first to explore this relationship as applied to ENSO. As shown and emphasized by those authors and later by Fedorov (2002) and Fedorov et al. (2003), this is *not* a conceptual model, but rather a nearly exact consequence of the primitive equations of motion and energy conservation as calculated for the tropical basin. Therefore, Eq. (1) has a universal character when applied either to general circulation models or to the appropriate measurements.

On interannual time scales, the perturbation available potential energy E is anticorrelated with sea surface temperatures in the eastern tropical Pacific so that negative values of E correspond to El Niño conditions, and positive values correspond to La Niña conditions (Fig. 1). This correlation is related to changes in the slope of the thermocline associated with El Niño and La Niña. When the thermocline slope increases (as during La Niña; Fig. 1a), the warmer and lighter water is replaced by colder and hence heavier water thus raising the center of mass of the system and increasing its gravitational potential energy. It is significant that the meridional redistribution of mass within the tropical band (as in the recharge–discharge mechanism of Jin 1997a,b) is taken into account by Eq. (1), but affects the APE only slightly.

In accordance with Eq. (1) variations in W lead those in E (Fig. 2b). If dissipation were truly negligible and this equation were precise, then variations in W would lead those in E by a quarter period, approximately on the order of 1 yr. The actual lag (roughly 6–9 months for major El Niño events) is significantly smaller, which implies finite dissipation in the system.

It is of interest to note that the latent heat lost by the ocean to the atmosphere, although of critical importance for the atmosphere, is of lesser importance for the energy balance of the ocean. In fact, net surface heat fluxes over the tropical box act as a linear damping on interannual and longer time scales (Boccaletti et al. 2004) and contribute to the dissipation term in Eq. (1). For instance, during the La Niña phase the ocean experiences additional net heat flux in the eastern Pacific

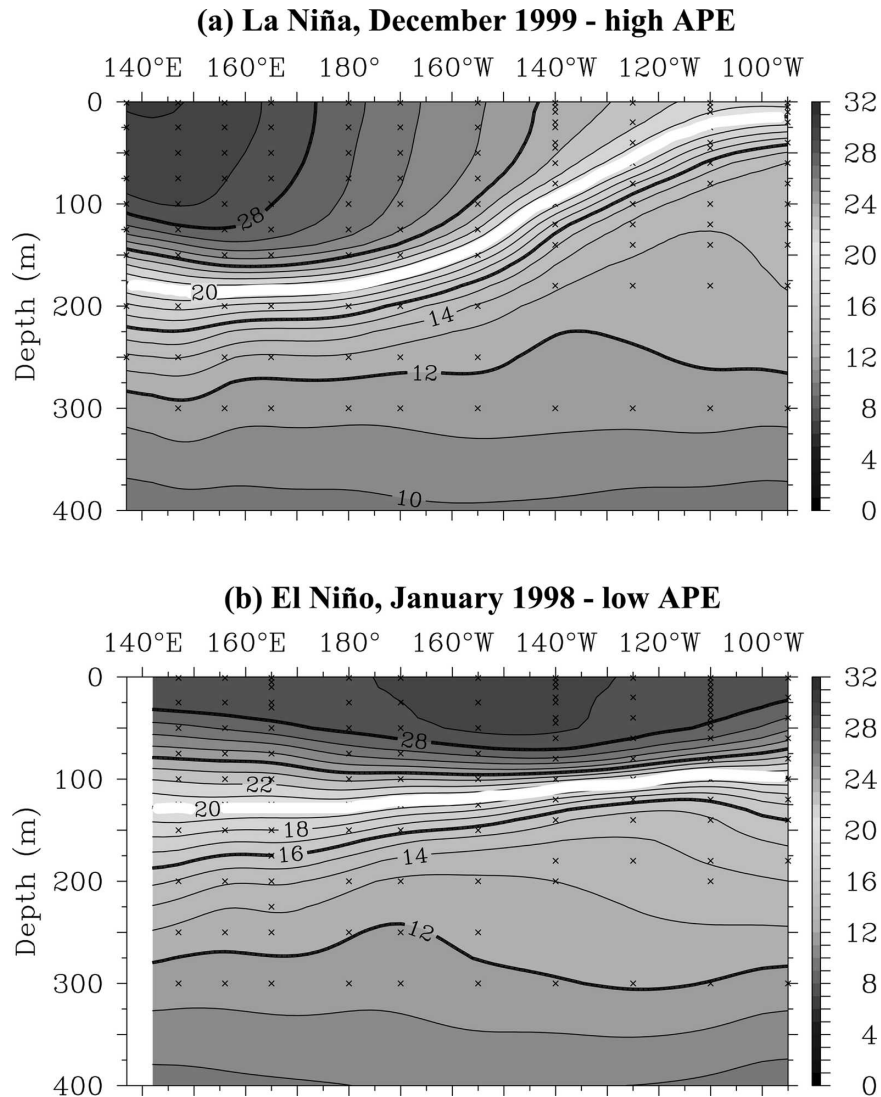


FIG. 1. Temperatures ($^{\circ}\text{C}$) as a function of depth along the equator at the peaks of La Niña and El Niño (from the TAO data; see McPhaden et al. 1998). El Niño is associated with low, La Niña with high APE. When thermocline slope increases, warmer and lighter water in the eastern equatorial Pacific is replaced by colder and heavier water thus raising the center of mass of the system and increasing its gravitational potential energy.

that tends to limit the shoaling of the thermocline there. (The diabatic heating of the atmosphere is obviously important for driving the winds in the Tropics and is taken into account indirectly when calculating the wind work.)

Also note that variations in the kinetic energy of the oceanic currents are negligible for the energetics on the time scales under consideration, as confirmed by Fig. 2c, which shows the relative magnitudes of the perturbation kinetic energy K and perturbation APE averaged over the tropical domain. [This is typical for baroclinic disturbances in the ocean. For example, Wunsch

(1998) estimated that the energy of oceanic baroclinic eddies is primarily potential and about 250 times larger than the kinetic energy.]

According to Eq. (1), because the dissipation in the system is relatively small, E and W are approximately in quadrature. This is why W and E can be used as phase coordinates. On a phase diagram that has as its horizontal and vertical axes W and E , respectively, an ENSO cycle is described by a counterclockwise trajectory that would normally pass through all four quadrants of the diagram to complete the cycle (Fig. 3, solid line). El Niño conditions correspond to the lower part

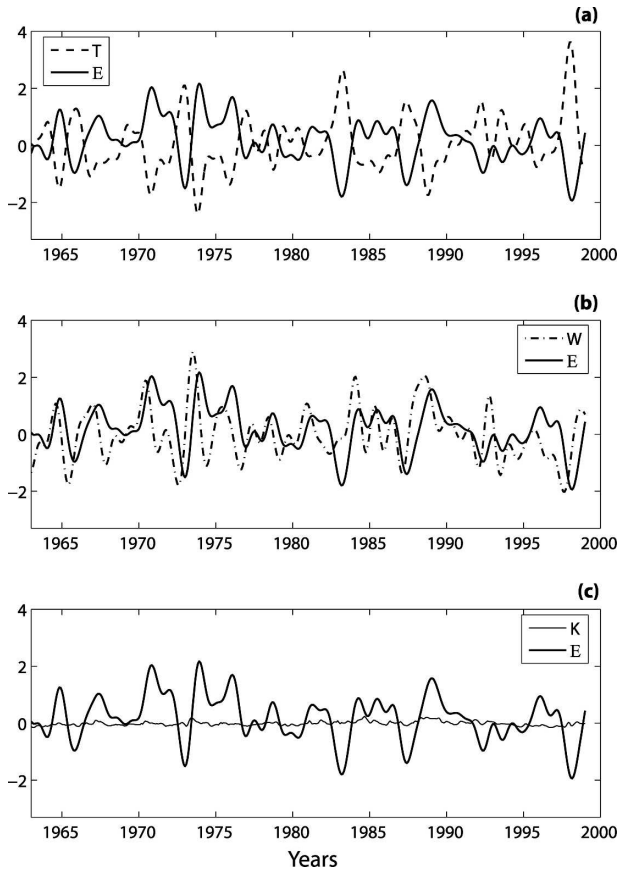


FIG. 2. (a) Variations in the sea surface temperature T of the eastern equatorial Pacific, and in the perturbation available potential energy E of the tropical ocean, for the period 1963–2000. The climatological seasonal cycle was subtracted from the original data. The correlation between T and E is -0.9 . (b) Variations in the wind work W and in the available potential energy E . The W leads E , for major El Niño events, by roughly 6–9 months. (c) Variations in E and kinetic energy K of the tropical ocean. Note the negligibly small values of K as compared to E . The E , W , and K time series are obtained by forcing a realistic high-resolution ocean GCM with the observed wind stress and heat fluxes, and then analyzing the density and velocity fields (see section 3 and appendix A). A low-pass filter with a cutoff frequency of 6 months was applied to the data. The units of E , W , and K are nondimensionalized.

of the diagram, and La Niña conditions correspond to the upper part. If the energy dissipation were large, the system's trajectory would collapse to a very narrow ellipse stretched along the horizontal axis.

The plot in Fig. 3 also shows changes in E and W due to the climatological annual cycle (dashed line, see appendix A), making it clear that the annual variations in the thermocline slope and available potential energy are relatively small. This is consistent with an occasionally overlooked observation that the thermocline depth in the eastern Pacific changes only slightly with the cli-

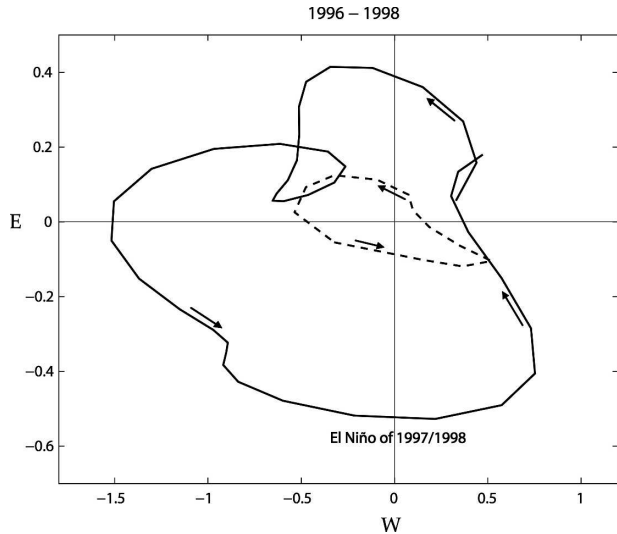


FIG. 3. A typical trajectory describing the location of the system on the E – W phase diagram showing roughly one ENSO cycle (solid line); the phase trajectory starts in September 1995 and ends in December 1998. The 1997/98 El Niño dominates the picture. For comparison, the trajectory associated with the climatological annual cycle is also shown (W_{cl} and E_{cl} , see appendix A). Variations in E_{cl} are relatively small (dashed line). The arrows indicate the direction of motion along the trajectories. Note that the trajectory of the climatological annual cycle is necessarily closed, but it is not so for the quasi-periodic interannual variability.

matological seasonal cycle (see, e.g., McPhaden et al. 1998; Zebiak and Cane 1987). Even such small changes in the thermocline depth may have a number of important physical implications as in Galanti et al. (2002). Overall, the dynamics of the seasonal cycle in the Tropics (e.g., Chang and Philander 1994) are rather different from those associated with ENSO and involve strong thermodynamic effects with direct forcing (heating) of the ocean by solar radiation and variations in the cross-equatorial winds, and as such are not considered in this paper.

Analyzing the difference (relatively small) between dE/dt and W from the data plotted in Fig. 2 shows that the most natural representation for the dissipation term in Eq. (1) is a linear function of energy E :

$$dE/dt = W - 2\alpha E. \quad (2)$$

The term $2\alpha E$ describes the fraction of the wind work lost to dissipation through various processes. This linear representation of dissipation has a simple physical meaning—all dissipation processes effectively tend to restore the state of the ocean toward the state with minimum perturbation APE. The greater anomalies associated with ENSO are, the stronger the restoring force is. Note that while Eq. (2) is linear, both energy and wind work are nonlinear variables (appendix A).

We will refer to α as the effective oceanic damping rate for thermocline anomalies (using an analogy with the shallow-water equations; see appendix B) and to 2α as the net energy dissipation rate in the tropical ocean. The thrust of this study is to estimate α^{-1} for different frequency bands, from subannual to nearly decadal. As we show later, α^{-1} is not exactly a constant but rather a function of the frequency band under consideration.

Finally, we should emphasize that the damping coefficient α does not describe the overall stability of the coupled system, since positive feedbacks due to ocean–atmosphere interactions should also be taken into account to do that. Thus, calculating α addresses only the oceanic part of the problem.

3. Estimating α

First, in order to calculate E and W , we have generated a high-resolution dataset of density ρ and the near-surface zonal current U as a function of depth, horizontal coordinates, and time. We use data from a realistic high-resolution ocean general circulation model, the Modular Ocean Model version 3 (MOM3) developed at the Geophysical Fluid Dynamics Laboratory (GFDL) forced by the observed winds and surface boundary conditions, similar to the approach adopted by Goddard and Philander (2000), Harper (2000), Fedorov et al. (2003), Li et al. (2001), and others. Variations in E and W calculated from this dataset over a 50-yr time interval are shown in Fig. 2.

Ideally, the calculations would be based on oceanic measurements assimilated into a realistic oceanic GCM, the way atmospheric datasets are generated for analyses of the dynamics and energetics of the atmosphere. The apparent difficulty in applying ocean reanalyses, however, is that most ocean data assimilation procedures do not conserve energy, and even those methods that tend to take care of energy conservation do allow arbitrary changes in the wind work. On the other hand, several tests with different ocean GCM have all consistently reproduced the energetics as described in Eq. (1).

The wind stress needed for forcing the GCM has a 1-month time resolution and provides reasonable spatial coverage. It was obtained by carefully matching the Comprehensive Ocean–Atmosphere Data Set (COADS) data (before 1993) with the winds from the NCEP atmospheric reanalysis for the years since 1993. The winds from NCEP were modified to match the main characteristics of COADS data before the year 1993 (i.e., within the time frame that both wind products were available).

To estimate α we implement the following procedure. Let us assume that E and W satisfy the balance of Eq. (2), $dE/dt = W - 2\alpha E$, and can be described by two monochromatic functions (strictly speaking we should apply the Fourier transform here, but this will not matter for the subsequent calculations):

$$W = W_o e^{i\omega t}; E = E_o e^{i\omega(t-\Delta)}, \quad (3)$$

where $\Delta = \Delta(\omega)$ is the lag between E and W (positive when W leads E), $\omega = 2\pi/T$ is the frequency, and T is the oscillation period. Here W_o and E_o are fixed amplitudes, both real numbers. If the damping coefficient α were zero, then W would lead E by a quarter period, and the value of the lag would be $\Delta = T/4$.

Substituting expressions (3) into Eq. (2) yields a compatibility condition connecting Δ , ω , and an arbitrary α :

$$\text{Im}[(i\omega + 2\alpha)e^{-i\omega\Delta}] = 0. \quad (4)$$

After a little algebra, one can solve Eq. (4) for Δ :

$$\Delta = (T/2\pi) \arctan(\pi/\alpha T). \quad (5)$$

This expression describes a theoretical curve $\Delta = \Delta(\alpha, T)$ that gives the lag Δ as a function of the period T and the damping coefficient α .

The same lag can be estimated from the data plotted in Fig. 2. To do so, we apply a narrow bandpass filter (centered at the frequency ω) to E and W . This procedure amounts to calculating expressions (3) empirically. Next, we calculate a frequency-dependent lag correlation $R = R(\omega, \Delta)$ as

$$R(\omega, \Delta) = \langle \widehat{E}(t - \Delta, \omega) \widehat{W}(t, \omega) \rangle / \langle \widehat{E}(t, \omega) \widehat{W}(t, \omega) \rangle. \quad (6)$$

Here, \widehat{E} is the result of applying the filter to $E = E(t)$, $\widehat{E}(t - \Delta, \omega)$ is the result of applying the filter to $E(t - \Delta)$, and the angle brackets $\langle \dots \rangle$ stand for a time averaging; a similar definition applies to $\widehat{W}(t, \omega)$. These calculations are relatively insensitive to the particular width or the structure of the bandpass filter, as long as the filter is narrow. The maximum (peak) value of R for each frequency would give the lag Δ as a function of ω or T obtained from the empirical data. Figure 4 shows the lag correlation $R(T, \Delta)$ and the theoretical curves $\Delta = \Delta(\alpha, T)$ for several values of α^{-1} .

A direct comparison shows that the best fit between the empirical result and the theoretical curve in the interannual frequency range (from 2 to 7 yr) is achieved for $\alpha^{-1} \approx 2.3$ yr. In the near-annual range (roughly

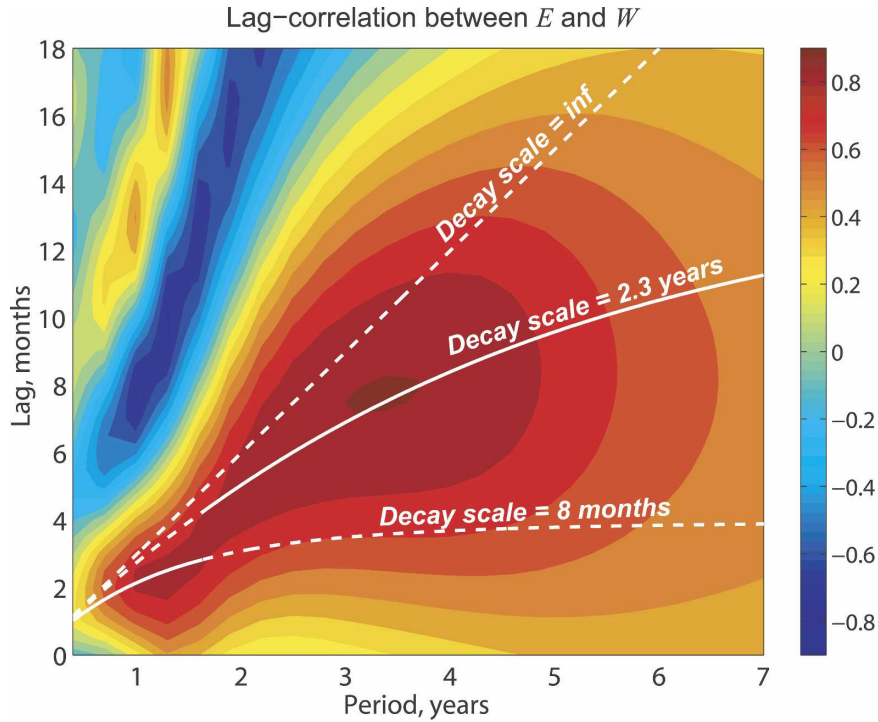


FIG. 4. The diagram showing the lag correlation $R = R(T, \Delta)$ between $\widehat{E} = \widehat{E}(t, \omega)$ and $\widehat{W} = \widehat{W}(t, \omega)$ as a function of the period T ($T = 2\pi/\omega$) and the lag Δ . In the interannual frequency range \widehat{W} leads \widehat{E} by 4–12 months. Several theoretical curves, calculated from Eq. (5) for different values of damping time scales α^{-1} , are also shown (white lines). In the interannual range the e -folding damping time scale is approximately 2.3 yr; in the near-annual range it is close to 8 months (these portions of the curves are indicated with solid lines). The inclined straight dashed line corresponds to zero net dissipation in the system (i.e., the damping time scale α^{-1} becomes infinitely long). The climatological annual cycle was subtracted from the initial values of E and W (see appendix A).

from 0.5 to 1.5 yr α^{-1} is approximately 8 months. The α^{-1} varies rapidly in the interval between 1.5 and 2 yr. Presumably, a larger relative loss of energy near the basin eastern boundary at shorter time scales (due to the generation of coastal Kelvin waves) is one of the factors that might explain two different dissipation regimes in Fig. 4.

It is easy to estimate the error bars for this method, since there is some leeway of how to fit a line into a relatively broad distribution. To do so, we plotted several additional theoretical curves in Fig. 4 for different values of α (not shown here) and estimated the range of α that would still give a reasonable fit for the graph. The results are $\alpha^{-1} = 2.3 \pm 0.4$ yr in the interannual range, and $\alpha^{-1} = 8 \pm 3$ months in the near-annual range, even though these error bars do not take into account a possible sensitivity of the results to changes in the input parameters of the ocean model. Note that if one tries to calculate an average value for the damping coefficient by fitting a theoretical curve over all avail-

able frequencies, he will arrive at a crude estimate of $\alpha^{-1} \approx 1.7$ yr, but this result clearly depends on how different parts of the spectrum are weighted.

4. Conclusions

We have estimated net energy dissipation rates in the tropical ocean in terms of characteristic damping time scale for the thermocline depth anomalies. We find two distinct dissipative regimes: in the interannual frequency band the damping time scale α^{-1} is approximately 2.3 yr; however, in the near-annual frequency band this time scale appears to be much shorter, roughly 8 months.

It is instructive to compare our results with the typical values of explicit damping coefficient α_s in the oceanic shallow-water equations used in intermediate coupled models, even though the two coefficients, α and α_s , are not identical (for a discussion see appendix B). Most of intermediate models such as the one by

Zebiak and Cane (1987) normally use $(2.5 \text{ yr})^{-1}$ for the damping coefficient α_s , which is close to our first estimate for α . Picaut et al. (1993) calculated much higher damping rates, with the decaying time scale of the order of 6 months to 1 yr, close to our second estimate. We hypothesize that it is the frequency dependence of damping and the difference between α and α_s that could explain how different estimates for α_s can diverge so much (since different estimating procedures can preferentially put more weight on different parts of the spectrum and/or do not distinguish between α and α_s).

What is the physical interpretation of α and its dependence on the frequency band under consideration? Suppose that the ocean is forced by oscillating sinusoidal wind stress with a fixed period. Such forcing should generate a certain amount of work per unit time (or power) fluctuating with the same period. In the absence of dissipation, all wind work would be utilized for inducing periodic changes in the slope of the thermocline (from large to small and back). The role of dissipation is to reduce the amount of work available for changing this slope and therefore reduce the range of the slope variations. Thus, the value of α indicates how much work will be irreversibly lost and how much will be available to modify the slope of the thermocline. If one repeats this experiment for different oscillation periods, it turns out that there are two distinct energy dissipation regimes: one when the ocean is forced at interannual, and one at near-annual frequencies. (This simple interpretation obviously circumvents the issue of possible energy exchange between lower and higher frequencies, which may become important.)

How robust are these results? It is true that ocean GCMs (with or without data assimilation) often lack representation of certain processes and do not resolve smaller or shorter scales important to dissipation. However, to the extent that the high-resolution ocean GCM that we used realistically describes the mean structure of the equatorial thermocline, oceanic stratification in the Tropics, equatorial upwelling, the structure of the Equatorial Undercurrent (all these characteristics being crucially dependent on dissipation), as well as their variations on interannual time scales (e.g., the amplitude and the structure of El Niño events), the modeling approach proposed here is relevant and physically sound. However, more studies are needed to establish how sensitive the diagram in Fig. 4 is to changes in the input parameters of the ocean model and the forcing data. With new datasets becoming available from measurements, the same approach can be easily extended to include those data.

What are the processes that control particular dissipation rates? There are three main mechanisms of en-

ergy dissipation in the tropical basin: internal dissipation via vertical and horizontal mixing (both explicit and eddy induced), negative thermodynamic feedbacks (shallower thermocline in the eastern Pacific implies stronger heat fluxes into the ocean), and energy loss through the northern, southern, and potentially western boundaries. This latter factor does include energy leakage through advection, but mostly it is the work that the volume of water contained within the tropical boundaries (as defined previously) should do on the surrounding fluid (i.e., the work of the ageostrophic component of normal pressure, see Goddard and Philander 2000). Our approach does not distinguish between these different dissipation mechanisms yielding only an integral quantity for dissipation. Currently, a series of sensitivity calculations are being made to determine the relative importance of different dissipation terms, including surface boundary conditions, parameterization of the vertical mixing, the model horizontal resolution, and the size of the integration domain. The results of these studies will be reported elsewhere.

The net dissipation as introduced here seems to be an important factor in the performance of coupled GCM. In a recent study by Guilyardi et al. (2004) several atmospheric GCMs were coupled with several ocean models in different combinations. This modular approach was used to investigate the respective roles of the ocean and atmosphere in controlling key El Niño properties in coupled calculations. Using this relatively limited ensemble of models, the authors came to a surprising conclusion: atmospheric GCMs determine the characteristic period of simulated ENSO; however, ocean GCMs still exert a large influence on setting the amplitude of El Niño. We can hypothesize that the latter factor can be attributed to the different net dissipation rates of the ocean models used by Guilyardi et al. (One could further speculate that the atmospheric models effectively set the strength of the positive atmospheric feedbacks in those calculations.) This suggests that the method presented in this paper can be used as an important diagnostic tool for coupled GCMs (specifically, their oceanic component). To that end, Fig. 4 could serve as a benchmark that coupled models should aim to reproduce. Preliminary calculations with several coupled models demonstrate that the gross features of Figs. 3 and 4 are indeed replicated by those models; however, there are strong quantitative and even qualitative differences between the models.

Another interesting conclusion from this study concerns intermediate climate modeling (also see appendix B). Our results from Fig. 4 suggest an intriguing possibility that rather than using a constant damping coefficient α_s in the shallow-water equations one may try to

use an operator α_s with appropriate properties in the frequency space, such that the damping should be stronger for shorter time scales. (This cannot be accomplished by solely increasing the damping for shorter spatial scales because most of intermediate models employ the long-wave approximation which filters out very short spatial scales, and because the motions with, say, 5- and 1-yr periods may have exactly the same spatial scales.) This remains a matter for future studies.

Acknowledgments. This research is supported in part by grants from NSF (OCE-0550439) and DOE Office of Science (DE-FG02-06ER64238), and by Yale University. I thank L. Goddard, S. Harper, J. Brown, and G. Philander for useful discussions, and A. Wittenberg for commenting on one of the first drafts of this paper.

APPENDIX A

Calculations of E and W

The full values of the available potential energy E and wind work W (strictly speaking, the rate or working or work per unit time) are calculated using the following expressions:

$$W = \iint U\tau dx dy; \quad E = \iiint \rho^2 dx dy dz, \quad (\text{A1})$$

$$\rho^2 = \frac{g(\rho - \rho^*)^2}{2 \left| \frac{\delta \rho^*}{\delta z} \right|}, \quad (\text{A2})$$

where $U = U(x, y, t)$ is the zonal current; $\tau = \tau(x, y, t)$ is the zonal wind stress; $\rho = \rho(x, y, z, t)$ is the local density; $\rho^* = \rho^*(z)$ is the hydrostatically balanced density profile; and g is the acceleration of gravity. The integration is conducted over the tropical Pacific domain (e.g., 15°N–15°S, 130°E–85°W), even though the dataset covers the entire Pacific basin, to the depth of some 400 m. A careful procedure should be implemented to eliminate the effect of the near-surface mixed layer where the vertical gradient of ρ^* vanishes (Goddard and Philander 2000). Preliminary calculations show that qualitative behavior of the energy and wind work time series does not change if the latitudinal extent of the domain is either reduced to 10° or increased to 20°.

Furthermore, it is assumed that the wind, zonal velocity, and $\hat{\rho}$ can be represented as a sum of climatological values and perturbations:

$$\tau = \bar{\tau} + \tau'; \quad U = \bar{U} + U'; \quad \hat{\rho} = \bar{\hat{\rho}} + \hat{\rho}'. \quad (\text{A3})$$

From this representation, E and W are calculated as

$$W = \iint \bar{U}\bar{\tau}' dx dy + \iint U'\bar{\tau} dx dy + \iint U'\tau' dx dy + \iint \bar{U}\bar{\tau} dx dy, \quad (\text{A4})$$

$$E = \iiint 2\bar{\hat{\rho}}\hat{\rho}' dx dy dz + \iiint (\hat{\rho}')^2 dx dy dz + \iiint (\bar{\hat{\rho}})^2 dx dy dz. \quad (\text{A5})$$

The climatological components of E and W [the last terms in (A4) and (A5)] are then subtracted from these expressions. The remaining perturbation values are plotted in Figs. 2 and 3 and then used for calculating the dissipation rates (we refer to those values as the perturbation APE and the perturbation wind work). The climatological values (W_{cl} and E_{cl}) are shown in Fig. 3 as a smaller 12-month cycle around the origin (the dashed line):

$$W_{cl} = \iint \bar{U}\bar{\tau} dx dy, \quad (\text{A6})$$

$$E_{cl} = \iiint (\bar{\hat{\rho}})^2 dx dy dz. \quad (\text{A7})$$

Note that in Fedorov et al. (2003) only the first term in (A5) and the first two terms in (A4) were used.

APPENDIX B

Relevance to the Shallow-Water Equations

A broad class of models used for studies and prediction of El Niño employ the reduced-gravity shallow-water equations for the ocean dynamics. These equations include “linear” dissipation in the form of Rayleigh friction in the momentum equations and a similar damping term in the continuity equation, which parameterizes turbulent mixing and modifies the thermocline depth. Frequently, the shallow-water equations are linearized and written in the long-wave approximation (e.g., Zebiak and Cane 1987; Battisti and Hirst 1989; Jin and Neelin 1993; Chang 1994; Wang et al. 1995; Tziperman et al. 1995; Moore and Kleeman 1999; Perigaud and Cassou 2000; Fedorov and Philander 2001; Fedorov 2002, and many others):

$$u_t + g^*h_x - \beta yv = \tau/\rho H - \alpha_s u, \quad (\text{B1})$$

$$g^*h_y + \beta yu = 0, \quad (\text{B2})$$

$$h_t + H(u_x + v_y) = -\alpha_s h. \quad (\text{B3})$$

The notations are conventional, with u and v denoting the ocean currents; h and H denoting the local and mean depth of the thermocline, respectively; τ is the zonal wind stress; g^* is the reduced gravity, etc. The subscripts t , x , and y indicate the respective derivatives. The meridional wind stress can be also added to the equations, but it plays only a minor role in the energy balance. The typical boundary conditions for this system are no flow ($u = 0$) at the eastern boundary and no net flow ($\int u \, dy = 0$) at the western boundary. (Note that the main conclusions of this paper are based on the full Navier–Stokes equations of motion, rather than the shallow-water equations.)

Following Gill (1980) and Cane and Patton (1984), in many applications it is assumed that the damping coefficient α_s has the same values in both continuity and momentum equations (which facilitates analytical treatment of this system), even though a priori the two coefficients are not required to be equal. This approach (i.e., adopting the same values for the damping coefficients) works fairly well as long as the damping is weak, and one needs to account for dissipation only in some average sense. In general, the ocean response appears to be more sensitive to the term in the continuity equation (e.g., Yamagata and Philander 1985). A question arises: what would be appropriate values of α_s to account for the tropical dissipation in a realistic setting?

Up to now attempts to estimate α_s remain scarce. Gent et al. (1983) found the damping scale of 2 yr for the fluctuations of ocean currents in the Indian Ocean. Zebiak and Cane (1987) adopted a value of 2.5 yr for α_s^{-1} in the Pacific Ocean. Following their study and those of Battisti (1988) and of Battisti and Hirst (1989) most of the intermediate coupled models assume the same time scale. More recently, Picaut et al. (1993) used available sea level height data from mooring stations, tide gauges, and the *Geosat* to constrain a shallow-water model [based on Eqs. (B1)–(B3)] and estimated much higher damping rates, with the decay time scale of the order of 6 months to 1 yr. Consequently, the preferred values for α_s vary from one study to the next.

It is clear that α_s in the shallow-water equations should be constrained, to a large degree, by α considered in this paper. In fact, after a series of simple transformations, integrating Eqs. (B1)–(B3) yields an equation similar to Eq. (2):

$$dE/dt = W - 2\alpha_s E + \text{Energy Loss at Boundaries}, \quad (\text{B4})$$

where

$$E = \frac{1}{2} \iint (Hu^2 + g^*h^2) \, dx \, dy, \quad (\text{B5})$$

and

$$W = \iint u\tau \, dx \, dy. \quad (\text{B6})$$

The kinetic energy component of (B5) is small for interannual variations. The integration in (B5) and (B6) is conducted over the tropical basin within the limits defined in appendix A. The term proportional to $2\alpha_s E$ describes explicit energy dissipation within the basin, while the term “Energy Loss at Boundaries” corresponds to the net loss of energy at the southern, northern, and western boundaries (it can be easily shown that the long-wave approximation and the requirement of no net flow at the western boundary imply energy leakage through that boundary). This additional term in (B4) describes an implicit energy loss in the system (in contrast to the explicit loss described by α_s); therefore, the damping coefficient α_s adopted for the use in shallow-water models should be necessarily smaller than α estimated in this paper (i.e., $\alpha_s^{-1} > \alpha^{-1}$).

REFERENCES

- Battisti, D. S., 1988: Dynamics and thermodynamics of a warming event in a coupled tropical atmosphere–ocean model. *J. Atmos. Sci.*, **45**, 2889–2919.
- , and A. C. Hirst, 1989: Interannual variability in a tropical atmosphere–ocean model: Influence of the basic state, ocean geometry and nonlinearity. *J. Atmos. Sci.*, **46**, 1687–1712.
- Boccaletti, G., R. C. Pacanowski, S. G. Philander, and A. V. Fedorov, 2004: The thermal structure of the upper ocean. *J. Phys. Oceanogr.*, **34**, 888–902.
- Cane, M. A., and R. J. Patton, 1984: A numerical-model for low-frequency equatorial dynamics. *J. Phys. Oceanogr.*, **14**, 1853–1863.
- Chang, P., 1994: A study of seasonal cycle of sea surface temperature in the tropical Pacific Ocean using reduced gravity models. *J. Geophys. Res.*, **99**, 7725–7741.
- , and S. G. H. Philander, 1994: A coupled ocean–atmosphere instability of relevance to the seasonal cycle. *J. Atmos. Sci.*, **51**, 3627–3648.
- Dijkstra, H. A., and J. D. Neelin, 1995: Ocean–atmosphere interaction and the tropical climatology. Part II: Why the Pacific cold tongue is in the east. *J. Climate*, **8**, 1343–1359.
- Fedorov, A. V., 2002: The response of the coupled tropical ocean–atmosphere to westerly wind bursts. *Quart. J. Roy. Meteor. Soc.*, **128**, 1–23.
- , and S. G. Philander, 2000: Is El Niño changing? *Science*, **288**, 1997–2002.
- , and —, 2001: A stability analysis of the tropical ocean–atmosphere interactions: Bridging measurements and theory for El Niño. *J. Climate*, **14**, 3086–3101.
- , S. L. Harper, S. G. Philander, B. Winter, and A. Wittenberg, 2003: How predictable is El Niño? *Bull. Amer. Meteor. Soc.*, **84**, 911–919.
- Galanti, E., E. Tziperman, M. Harrison, A. Rosati, R. Giering, and Z. Sirkes, 2002: The equatorial thermocline outcropping—A seasonal control on the tropical Pacific ocean–atmosphere instability strength. *J. Climate*, **15**, 2721–2739.

- Gent, P. R., K. O'Neill, and M. A. Cane, 1983: A model of the semi-annual oscillation in the equatorial Indian Ocean. *J. Phys. Oceanogr.*, **13**, 2148–2160.
- Gill, A. E., 1980: Some simple solutions for heat-induced tropical circulation. *Quart. J. Roy. Meteor. Soc.*, **106**, 447–462.
- Goddard, L., and S. G. H. Philander, 2000: The energetics of El Niño and La Niña. *J. Climate*, **13**, 1496–1516.
- Guilyardi, E., and Coauthors, 2004: Representing El Niño in coupled ocean–atmosphere GCMs: The dominant role of the atmospheric component. *J. Climate*, **17**, 4623–4629.
- Harper, S., 2000: Thermocline ventilation and pathways of tropical subtropical water mass exchange. *Tellus*, **52A**, 330–345.
- Jin, F.-F., 1997a: An equatorial ocean recharge paradigm for ENSO. Part I: Conceptual model. *J. Atmos. Sci.*, **54**, 811–829.
- , 1997b: An equatorial ocean recharge paradigm for ENSO. Part II: A stripped-down coupled model. *J. Atmos. Sci.*, **54**, 830–847.
- , and J. D. Neelin, 1993: Modes of interannual tropical ocean–atmosphere interaction—A unified view. Part I: Numerical results. *J. Phys. Sci.*, **50**, 3477–3503.
- Kessler, W. S., 2002: Is ENSO a cycle or a series of events? *Geophys. Res. Lett.*, **29**, 2125, doi:10.1029/2002GL015924.
- Li, X., Y. Chao, J. C. McWilliams, and L.-L. Fu, 2001: A comparison of two vertical mixing schemes in a Pacific Ocean general circulation model. *J. Climate*, **14**, 1377–1398.
- McPhaden, M. J., and Coauthors, 1998: The tropical ocean global atmosphere observing system: A decade of progress. *J. Geophys. Res.*, **103**, 14 169–14 240.
- Moore, A. M., and R. Kleeman, 1999: Stochastic forcing of ENSO by the intraseasonal oscillation. *J. Climate*, **12**, 1199–1220.
- Oort, A. H., S. C. Ascher, S. Levitus, and J. P. Peixoto, 1989: New estimates of the available potential energy in the world ocean. *J. Geophys. Res.*, **94**, 3187–3200.
- Perigaud, C. M., and C. Cassou, 2000: Importance of oceanic decadal trends and westerly wind bursts for forecasting El Niño. *Geophys. Res. Lett.*, **27**, 389–392.
- Philander, S. G., and A. V. Fedorov, 2003: Is El Niño sporadic or cyclic? *Annu. Rev. Earth Planet. Sci.*, **31**, 579–594.
- Picaut, J., C. Menkes, J.-P. Boulanger, and Y. du Penhout, 1993: Dissipation in a Pacific equatorial long-wave model. *TOGA Notes*, No. 10, IRD, Paris, France, 11–15.
- Thompson, C. J., and D. S. Battisti, 2000: A linear stochastic dynamical model of ENSO. Part I: Model development. *J. Climate*, **13**, 2818–2832.
- , and —, 2001: A linear stochastic dynamical model of ENSO. Part II: Analysis. *J. Climate*, **14**, 445–466.
- Tziperman, E., M. A. Cane, and S. Zebiak, 1995: Irregularity and locking to the seasonal cycle in an ENSO prediction model as explained by the quasi-periodicity route to chaos. *J. Atmos. Sci.*, **52**, 293–306.
- Wang, B., T. Li, and P. Chang, 1995: An intermediate model of the tropical Pacific Ocean. *J. Phys. Oceanogr.*, **25**, 1599–1616.
- , S.-P. Xie, and J. A. Carton, Eds., 2004: *Earth's Climate: The Ocean–Atmosphere Interaction*. *Geophys. Monogr.*, Vol. 147, Amer. Geophys. Union, 405 pp.
- Wunsch, C., 1998: The work done by the wind on the oceanic general circulation. *J. Phys. Oceanogr.*, **28**, 2332–2340.
- , and R. Ferrari, 2004: Vertical mixing, energy, and the general circulation of the ocean. *Annu. Rev. Fluid Mech.*, **36**, 281–314.
- Yamagata, T., and S. G. Philander, 1985: The role of damped equatorial waves in the oceanic response to winds. *J. Oceanogr. Soc. Japan*, **41**, 345–357.
- Zebiak, S. E., and M. A. Cane, 1987: A model El Niño–Southern Oscillation. *Mon. Wea. Rev.*, **115**, 2262–2278.